CONF-900331--13

DE90 015541

Investigation into the Feasibility of a Soft Muon Experiment

Mark L. Tincknell

Oak Ridge National Laboratory

Oak Ridge, Tennessee 37831-6372

May 21, 1990

Abstract

Issues relevant in a soft (< 5 GeV) muon pair experiment at the AGS or the RHIC central region are investigated. Observation of direct muon pairs is difficult because the muon pair to pion ratio is $\mathcal{O}(10^{-4})$. Absorber penetration is the only means available to identify high energy muons among a large number of hadrons. Three important sources of background are sail-through hadrons that fail to interact in the absorber, the decays of pions and kaons to muons in the absorber, and leakage of hadronic shower products through the absorber. An absorber thick enough to limit the ratio of combinatorical background pairs to pions to $\mathcal{O}(10^{-4})$ imposes a significant muon kinetic energy threshold due to muon range in the absorber. Absorbers with low atomic number Z are preferred to keep this threshold low, and to avoid loss of invariant mass resolution due to energy loss straggling and multiple coulomb scattering. Long-lived meson to muon decays can be directly suppressed only by picking an absorber with short interaction length, which implies a high density, high Z material. With sufficiently high statistics, a subtraction of the spectra of like-sign pairs from the spectrum of opposite-sign pairs should recover the direct muon pair spectrum.

Direct photons and lepton pairs are interesting probes of hadronic collision processes because they do not have significant final state interactions. Unfortunately, the same characteristic weakness of interaction suppresses their yield relative to produced hadrons, handicapping their usefulness. The direct photon signal is all but overwhelmed by the

copious production of background photons from $\pi^0 \rightarrow 2\gamma$ decays. Dielectrons must be detected amid a huge background of charged hadrons, and "interesting" electron pairs must be distinguished from $\pi^0 \rightarrow \gamma e^+e^-$ decays, and $\gamma + Z \rightarrow e^+e^- + Z$ conversions. This motivates the study of dimuons, for which the lack of hadronic interactions again can be used advantageously to identify them from background hadrons. All high energy physics experiments which study muons use absorbers to filter out hadrons and identify the penetrating particles as muon candidates. Very few high energy physics experiments have studied muons below a muon kinetic energy of ~5 GeV [1]. The central rapidity region of Au + Au collisions at AGS fixed target energies (11.9 AGeV/c) is at rapidity 1.62, and the central rapidity region at RHIC energies (100 + 100 AGeV/c) is at rapidity $|y| \lesssim 1$. Most direct muons from these sources will have kinetic energies < 2 GeV. The dimuons produced in these kinematic regions could yield extremely interesting information about the collision processes, if the muons can be identified. The purpose of this article is investigate whether soft ($\lesssim$ 5 GeV) muons can be studied experimentally in either of these domains.

There are two main sources of "interesting" dimuon production:

- the decay of massive virtual photons, and
- the decay of neutral vector mesons, namely the ρ, ϕ, and J/ψ.

The Feynmann diagram for virtual photon production and decay contains two electromagnetic vertices, one for the emission of the photon from a charged hadron current, and the other for the decay of the photon into the $\mu^+\mu^-$ pair. Semi-quantitatively, each vertex contributes one power of the fine structure constant α to the rate, so the order of magnitude of the overall rate for the process is $\mathcal{O}(\alpha^2) = 1/137^2 = 5.3 \times 10^{-5}$. The production cross section for ρ mesons in hadronic collisions is ~ mb, but the branching ratio (B.R.) for $\rho \rightarrow \mu^+\mu^-$ is 6.7×10^{-5}. The cross section for ϕ production is < mb, and the B.R. is 2.5×10^{-4}. The B.R. for $\psi \rightarrow \mu^+\mu^-$ is 7.4×10^{-2}, but the production cross section is < μb. Experimentally, the ratio of muon pair to pion production is observed to be $\mu^+\mu^-/\pi \lesssim 10^{-4}$ for almost every energy and colliding system measured [1,2]. This means that the muon identification in any soft muon experiment must reject oppositely-charged pairs of background particles at the level of $\lesssim 10^{-4}$ just to provide a 1:1 signal to background ratio.

The experimental definition of a muon is a minimum ionizing particle that does not interact hadronically or shower electromagnetically. This is the only characteristic that

can be used to discriminate between high energy muons and charged pions, because the muon mass is 75.7% of the charged pion mass. To understand why other methods of particle identification cannot help, consider the example of time-of-flight *vs.* momentum identification. A formula for the maximum momentum the muon candidate could have and still allow a pion to be rejected by time-of-flight is

$$p_{max} \leq \left[\frac{xc\beta^2(m_\pi^2 - m_\mu^2)}{2\Delta t_{res}} \right]^{1/2}. \tag{1}$$

An AGS experiment with a flight path of 8 m, and a 5σ Δt of 400 ps, has $p_{max} \leq 530$ MeV/c. This momentum range is too low to identify the muons from the symmetric decay of a mid-rapidity ($y = 1.62$) ρ meson, where each muon has momentum 1005 MeV/c. Note also that 23.7% of 530 MeV/c pions will decay into muons within an 8 m flight path. These factors force a soft muon experiment to use the traditional principle of muon identification, a hadron absorber.

There are three obvious sources of background for a soft muon experiment:

- sail-through hadrons which fail to interact in the absorber,
- secondary muons from the long-lived meson decays $\pi \rightarrow \mu\nu$ and $K \rightarrow \mu\nu$, and
- secondary hadronic shower particles that leak through the absorber.

This article will explore the consequences of the first two of these backgrounds, the sail-throughs and the long-lived decays. The third background, leak-throughs, is the subject of RHIC R&D Experiment RD10 [3], since it is impossible to calculate or model that process to the desired level of accuracy, $\mathcal{O}(10^{-4})$.

To what level must all the backgrounds (from sail-through hadrons, long-lived meson decays, and leak-through shower particles) be reduced? Let w be the probability that a hadron causes a fake muon candidate by any of the background mechanisms. If there are N hadrons in an event in the acceptance of the experiment, then the probability that n of them fake muons in that event is given by the binomial probability distribution,

$$\mathrm{p}(n) = \frac{N!}{n!(N-n)!} w^n (1-w)^{N-n}. \tag{2}$$

The probability that $n \geq 1$ is $1 - \mathrm{p}(0) \approx Nw$ for small w. The dimuon signal is actually *a pair of muon candidates of opposite charge.* Assume that the probability of a real $\mu^+\mu^-$ pair is $\zeta \approx 10^{-4}$ per hadron, and (approximating the binomial distribution again),

the number per event is $\approx N\zeta$. The probability of 1 or more fake pairs in an event is (prob. of $n^+ \geq 1$) $\times$ (prob. of $n^- \geq 1$) $\approx (N^+w)(N^-w) = N^+N^-w^2$. Assuming that $N^+ = N^- = N/2$, then for a 1:1 signal to background ratio, $N\zeta = N^+N^-w^2 = N^2w^2/4$. Thus the limit on w is

$$w \leq 2(\zeta/N)^{1/2}. \tag{3}$$

For $N = 100$, $w \leq 2 \times 10^{-3}$, and for $N = 1000$, $w \leq 6.3 \times 10^{-4}$. These numbers are the goals background rejection must strive to achieve.

Hadronic interactions exponentially attenuate the hadron flux penetrating an absorber. Disregarding hadronic secondaries generated by interacting hadrons, the fraction of hadrons that exit the absorber without interacting is $\exp(-x/\lambda)$, where x/λ is the absorber thickness in interaction lengths. For a $\mu^+\mu^-/\pi$ ratio of $\zeta \approx 10^{-4}$, and number of hadrons per event of $N \approx 400$, the minimal criterion from Eq. (3) requires that $w = \exp(-x/\lambda) \lesssim 10^{-3}$. This means that the absorber thickness must be $x/\lambda \gtrsim 6.9$, so that sail-through hadron pairs are attenuated to the same flux level as the direct muon signal. Muons penetrating an absorber do not interact hadronically, but they do lose energy continuously by dE/dx, exciting or ionizing atoms in the absorber. Soft muons will range out and stop in a sufficiently thick absorber, but if they do not penetrate far enough, discrimination against hadrons is impossible. Thus muons must have a minimum kinetic energy to penetrate at least 7 interaction lengths of material; that kinetic energy depends on the absorber material's atomic properties. Figure 1 shows the average range of a muon in interaction length units as a function of muon kinetic energy for three absorber materials: beryllium (Be), carbon (C), and copper (Cu). Figure 2 shows the exponentially decreasing probability that a hadron can sail through an absorber just thick enough to range out muons of kinetic energy given on the abscissa. This figure shows that to achieve $w < 10^{-3}$ for sail-throughs alone, muons must have kinetic energy > 900 MeV for a Be absorber, K.E. > 1100 MeV for a C absorber, and for Cu, K.E. > 1450 MeV. Absorbers with higher atomic number than Cu ($Z = 29$), have even higher kinetic energy cut-offs.

To understand the effect of these kinetic energy cut-offs on experimental observables, consider the example of vector mesons produced at mid-rapidity in AGS fixed-target collisions. Assume that the mesons have mass M, $p_\perp = 0$, and that they decay symmetrically into equal energy muons in the lab frame. In the meson rest frame, the muons share equally the energy available, so the total relativistic energy of each is $E_\mu = M/2$. In the lab frame, each muon has total energy $E'_\mu = E_\mu \cosh y$, where y was the mesons' rapidity. At mid-rapidity at the AGS, $y = 1.62$, the muons from ρ mesons (mass 770 MeV) each

have kinetic energy 906 MeV, marginal to penetrate even the Be absorber. Practically, this means that a muon experiment is incapable of observing low-$p_\perp$ ρ mesons at mid- or lower rapidity at the AGS. With a 7λ C absorber, $p_\perp = 0$ $\rho \rightarrow \mu^+\mu^-$ decays could be observed only for rapidities $y \geq 1.80$, and the rapidity threshold for $p_\perp = 0$ $\phi \rightarrow \mu^+\mu^-$ decays is $y \geq 1.50$. Muons from the decay of a mid-rapidity, $p_\perp = 0$, ψ meson (mass 3100 MeV) each have ample kinetic energy, 3965 MeV; however the kinematic production threshold for the ψ in fixed-target p-p collisions is 12200 MeV/c, so ψ production is very small at AGS energies.

Note also that the kinetic energy of each of the muons from the decay of a $y = 0$, $p_\perp = 0$, ψ in the central region at RHIC is 1444 MeV, borderline to penetrate a realistic absorber in a cylindrical detector. This implies that the detection efficiency of a muon experiment at RHIC for $\psi \rightarrow \mu^+\mu^-$ decays will be poor for small y, low $p_\perp$ ψ's, and that the efficiency will be strongly $p_\perp$- and y-dependent. Dimuons with invariant mass below the ψ will be essentially unidentifiable in the central region. More specific statements require detailed study of the rates of signal and background for particluar detector geometries as a function of rapidity y, transverse momentum $p_\perp$, and invariant mass M.

The absorber also has a serious impact on the quality of the muon momentum measurement. The invariant mass of the muon pair is

$$\begin{aligned} M &= \left[(E_{\mu 1} + E_{\mu 2})^2 - |\mathbf{p}_{\mu 1} + \mathbf{p}_{\mu 2}|^2\right]^{1/2}, \\ &= \left[2m_\mu^2 + 2(E_{\mu 1}E_{\mu 2} - p_{\mu 1}p_{\mu 2}\cos\theta_{12})\right]^{1/2}, \end{aligned} \tag{4}$$

where E_μ is the total energy of a muon, $\mathbf{p}_\mu$ (p_μ) is the muon's momentum (magnitude), m_μ is the muon mass, and θ_{12} is the angle between the muons. For a symmetric decay with muon pair $p_\perp = 0$, and $\theta' = \theta_{12}/2$ (half the lab angle between the muons), the fractional invariant mass resolution is

$$\frac{\Delta M}{M} = \left[\left(\frac{\Delta p}{p}\right)^2 + \left(\frac{\Delta\theta'}{\tan\theta'}\right)^2\right]^{1/2}. \tag{5}$$

Δp is experimental uncertainty in the muon's momentum, due to measurement accuracy and energy loss straggling (ELS) in the absorber, and $\Delta\theta'$ is the uncertainty in the half-angle between the muons, due to measurement limitations and multiple coulomb scattering (MCS). ELS is proportional to the total energy the muons lose in the absorber, which is greater for absorbers with large atomic number. The mean MCS angle is also approximately proportional to the atomic number Z of the absorber.

In order to quantify the effect of ELS and MCS on mass resolution, a series of simple GEANT simulations were done [4]. Muons of several kinetic energies (2, 5, 10, and 20 GeV) were shot through several kinds of absorber (Be, C, and Cu) of various thicknesses ($\sim 3\lambda$, $\sim 5\lambda$, and $\sim 7\lambda$). The distributions of muon momentum and angle on exit from the absorber were accumulated. In Fig. 3 are ELS histograms of $|p_{peak} - p_{exit}|/|p_{peak}|$ for 1500 Monte Carlo muons of 2000 MeV K.E. incident on three absorbers: 4.5λ Be, 3.9λ C, and 2.9λ Cu. In Fig. 4 are muon exit angle distributions for the same three absorbers. The histograms in both Figs. 3 and 4 were smoothed to compensate for low statistics. These distributions were then used to determine values for Δp and $\Delta\theta'$ in Eq. (5). Fig. 5 shows the fractional invariant mass resolution for two cases of invariant mass (ρ meson, mass 770 MeV, and ψ meson, 3100 MeV), and three absorbers (4.5λ Be, 3.9λ C, and 2.9λ Cu), for meson kinetic energies ranging from 1 to 19 GeV. The fractional resolution in all cases is below 0.12, and in all but one case less than the fractional intrinsic width of the ρ, 0.085.

The rationale for using such thin absorbers in these examples is to try to preserve as much resolution as possible. One possible experimental configuration would divide the total thickness of absorber into two parts: the first part between the target (or interaction region) and the momentum analyzer, and the second part following the analyzer to complete the thickness needed for confident muon identification. The first absorber would only need to be thick enough to attenuate the hadron flux down to a level which the tracking in the momentum analyzer could handle without confusion. This could be approximately half the total absorber thickness, resulting in nearly twice as good mass resolution as tracking after the full absorber. The experiment would be triggered by two or more muon candidates penetrating the second absorber to a sufficient depth. Because there is no tracking after the full absorber, the kinetic energy of muons is efficiently expended reaching the minimum absorber depth required, giving the lowest possible kinetic energy threshold.

Probably the most serious backgrounds confronting a soft muon experiment are the decays $\pi \rightarrow \mu\nu$ and $K \rightarrow \mu\nu$. The production of muons from the decay of mesons *in an absorber* can be described by the pair of simple differential equations,

$$\begin{aligned} \frac{d\mathcal{F}}{dx} &= (-1/\lambda - 1/\tau)\mathcal{F} \\ \frac{d\mathcal{M}}{dx} &= (+\alpha/\tau)\mathcal{F}, \end{aligned} \tag{6}$$

where $\mathcal{F}$ is the flux of mesons, $\mathcal{M}$ is the flux of muons, λ is the mean free path of the

mesons, $\tau = c\beta\gamma\tau_0$ is the lab distance equivalent to the meson lifetime, and α is the branching ratio for the meson to muon decay. Solving these equations, the integrated muon yield (neglecting decay of the muons themselves) for an absorber of thickness x, is

$$\mathcal{M} = \frac{\alpha \mathcal{F}_0}{(\tau/\lambda + 1)}\{1 - \exp[-x(1/\lambda + 1/\tau)]\}, \tag{7}$$

where $\mathcal{F}_0$ is the initial meson flux. In Fig. 6, the probabilities (on a log scale) for π and K mesons to decay to muons are given for the range of meson kinetic energies along the abscissa, 0 – 20000 MeV. The four curves correspond (in descending order) to kaons in a Be absorber, kaons in Cu, pions in Be, and pions in Cu. It is more probable for kaons to decay than pions because kaons have a shorter lifetime, 12 ns *vs.* 26 ns for pions, and a smaller time dilation factor γ at a given K.E. (although the branching ratio to muons is only 63.5% for kaons, whereas it is virtually 100% for pions). The probabilities for decay are lower in Cu than Be because λ is shorter in Cu and the mesons are more likely to interact in a given decay length in Cu than in Be. The probabilities are not drawn for low meson kinetic energy, because muons from the decays of such mesons have too little energy to penetrate a $\sim 7\lambda$ absorber.

The only optimization available to the experimenter in Eq. (7) is to make the ratio τ/λ as large as possible. For high energy muon experiments, τ is long because of relativistic time dilation, but this advantage is unavailable by definition to a soft muon experiment. The requirement that λ be as short as possible demands a high density absorber material. Unfortunately, high density materials invariably have a high atomic number Z, with accompanying high ELS and MCS to the detriment of resolution, and high total dE/dx energy loss which raises the muon kinetic energy threshold. The experimenter must trade off these incompatible criteria when choosing an absorber material.

In Tables 1 and 2 are listed properties of 31 low-Z absorber candidates [5,6]. The list excludes organic materials, because all organic materials have density $\rho \leq 1.3$ g/cm^3, which gives them distressingly high probabilities for long-lived meson to muon decay. Properties listed include the density ρ, radiation length X_0, hadronic interaction length λ, range R of a 2000 MeV (K.E.) muon, energy loss ΔE of a 2000 MeV muon penetrating 9λ of absorber, the mean MCS angle θ_{MCS} of a 2000 MeV muon, and the probabilities P(π) and P(K) for a 2000 MeV π or K meson to decay to a muon before interacting in 9λ of absorber. Be is an excellent material for reducing ELS and MCS, but its price is about $500. per pound [7]. BeO might be a good candidate for the first absorber material, since it has the same effective atomic number as C, and > 1.3 times the density; unfortunately

BeO costs approximately \$275. per pound [7]. The cost of $\rho = 1.72$ g/cm^3 C (CS grade graphite) is about \$2.33 per pound, and the cost of $\rho = 2.0$ g/cm^3 C (ZTA aerospace grade) is about \$50. per pound ($\rho = 2.25$ g/cm^3 C is not readily available) [8]. Al_2O_3 might be a good material for the second absorber, since it is almost 50% denser than Al, and has a lower effective atomic number.

The kinematics of *meson* $\rightarrow \mu\nu$ decays exhibit several important features. In the meson rest frame, the total muon energy is $E_\mu = (M^2 + m_\mu^2)/(2M)$, and the muon momentum is $|\mathbf{p}_\mu| = p_\mu = (M^2 - m_\mu^2)/(2M)$, where M is the meson mass and m_μ is the muon mass. In the lab frame,

$$\begin{aligned} E'_\mu &= \gamma(E_\mu + \beta p_\mu \cos\theta), \text{ or} \\ \cos\theta &= (E'_\mu/\gamma - E_\mu)/(\beta p_\mu), \end{aligned} \tag{8}$$

where γ and β are the Lorentz factors for the meson (the boost), and θ is the angle between the meson direction and the muon direction in the meson rest frame. θ is random, and in the meson frame, $\cos\theta$ is uniformly distributed because π and K mesons have spin 0, so the probability law is

$$\mathrm{p}(\theta)d\theta = \frac{\sin\theta d\theta}{2} = \frac{d(\cos\theta)}{2} = \frac{dE'_\mu}{2\beta\gamma p_\mu}. \tag{9}$$

Thus the muon total lab energy E'_μ is also uniformly distributed, between $E'_{min} = \gamma(E_\mu - \beta p_\mu)$ and $E'_{max} = \gamma(E_\mu + \beta p_\mu)$; $E'_{min}/E_\pi \approx 0.57$ and $E'_{min}/E_K \approx 0.046$. In Fig. 7 are shown the probability distributions of muon lab kinetic energy for six cases: $\pi \rightarrow \mu\nu$ for 2000, 5000, and 10000 MeV K.E. pions, and K $\rightarrow \mu\nu$ for 2000, 5000, and 10000 MeV K.E. kaons.

The probability distribution law for the lab angle θ' between the meson direction and the muon direction is quite complicated. In particular, if the meson $\beta > (M^2 - m_\mu^2)/(M^2 + m_\mu^2)$, then there are two angles θ in the meson rest frame that correspond to the same θ' in the lab, and there is a maximum lab angle given by

$$\tan\theta'_{max} = \frac{p_\mu}{\gamma(\beta^2 E_\mu^2 - p_\mu^2)^{1/2}}. \tag{10}$$

The probability distribution $\mathrm{p}(\theta')d\theta'$ *diverges* at θ'_{max} (although $\int \mathrm{p}(\theta')d\theta' = 1$ of course). In Figs. 8 and 9 are shown the probability distributions for the lab angle between the meson direction and the muon direction, for pions and kaons of kinetic energies 2000, 5000, and 10000 MeV.

One simple strategy to reject some of the *meson* $\rightarrow \mu\nu$ decays is to cut on muons that do not point to the interaction vertex. The mean muon momentum transverse to the meson direction is $<p_\perp> = (\pi[M^2 - m_\mu^2])/(8M)$, and the mean muon momentum along the meson direction is $<p_{||}> = (\beta\gamma[M^2 + m_\mu^2])/(2M)$. Thus the mean lab angle θ' is

$$<\theta'> \approx <\tan\theta'> = \left\langle \frac{p_\perp}{p_{||}} \right\rangle \approx \frac{<p_\perp>}{<p_{||}>} = \frac{\pi[M^2 - m_\mu^2]}{4\beta\gamma[M^2 + m_\mu^2]}. \tag{11}$$

A formula for the mean MCS angle for muons is $\theta_{MCS} = \{0.134/(\beta^2\gamma)\}[x/X_0]^{1/2}$, for an absorber x/X_0 radiation lengths thick. The ratio of these two angles is

$$\frac{<\theta'>}{\theta_{MCS}} = \begin{cases} 1.62\beta[X_0/x]^{1/2}, & \text{for } \pi \rightarrow \mu\nu \\ 5.34\beta[X_0/x]^{1/2}, & \text{for K} \rightarrow \mu\nu. \end{cases} \tag{12}$$

Even for a 4.5λ Be absorber, $[x/X_0]^{1/2} = 2.3$, and the ratio in Eq. (12) for $\pi \rightarrow \mu\nu$ is < 1: the mean decay angle is completely obscured by the MCS angle. This approach does not work.

Another, more complicated method to reduce the *meson* $\rightarrow \mu\nu$ background is to measure the particle momentum before it has a chance to decay, and compare that to a second momentum measurement made downstream of absorbers which identify the particle as a muon. If the two momenta agree, then the probability is reduced that the muon originated from a long-lived meson decay between the two measurements. This method can be called double momentum analysis. Consider an experimental configuration consisting of a first absorber immersed in a first magnetic field, followed by tracking in a second magnetic field in an absorber-free region, followed by a second absorber thick enough to complete muon identification. Assuming that all particles originate from the vertex (and do not decay before they are bent appreciably), the position and direction at the exit point of the first absorber give the first momentum measurement. The arc in the second magnetic field (in the absorber-free region) gives the second momentum measurement. If the second absorber is instrumented at regular depth intervals, then the end of range of slow particles gives a total energy that can be used as a third measurement that must agree with the other two.

What power does this scheme have to reject background? The accuracy of the first momentum measurement is limited by MCS in the first absorber. Consider an example configuration consisting of a first absorber of 1.83 m of Be (4.5λ) in a 1.5 T magnetic field. An analytic study was made, assuming the average MCS angle is given by the usual analytic formula, $\theta_{MCS} = 14.1(\text{MeV}/c)[x/X_0]^{1/2}/(p\beta)$. The MCS-limited momentum resolution obtained was $\Delta p/p = \{+0.090, -0.075\}$, for both $p = 2000$ and 5000 MeV/c.

This ratio is independent of p (to first order), because the momentum measurement essentially involves measuring the lateral distance between the exit point and a straight-line (no curvature) exit point; this distance is proportional to $1/p$. The MCS angle also goes like $1/p$, so in the ratio $\Delta p/p$, the momentum dependences cancel to first order. For comparison, the momentum deduced from the "average" decay of a 2135 MeV/c π into a 1675 MeV/c μ half way (0.92 m) through the absorber was also calculated. Using the muon exit point and exit angle from the absorber, the apparent momentum of the muon, if it were coming directly from the interaction vertex, was only 3.4% to 7.7% greater than the actual 1675 MeV/c momentum the second momentum analyzer would find. This is within the 9% momentum resolution of the first measurement, so it would be impossible to reject this particle as a muon from meson decay in the absorber. Although more study is needed, this background rejection scheme is not very promising either.

In any soft muon experiment in a high multiplicity environment, the signal to background ratio will not be large, so a statistical correction for the background will have to be made. The spectrum of detected pairs will be composed of like-sign and unlike-sign pairs in not-quite-equal numbers. Can the real $\mu^+\mu^-$ spectrum still be extracted, with sufficiently high statistics, by subtracting the like-sign spectrum from the unlike-sign spectrum? Let $N_{\pi\pm}$ and $N_{\mathrm{K}\pm}$ be the numbers of pions and kaons per event, and let q_π and q_K be the probabilities that they contribute fake muon candidates (primarily from $\mu\nu$ decay). Assume that $N^{+-} = N_{\mu\mu} + N^{+-}_{fake}$, *i.e.* the total number of candidate pairs in an event is the sum of the real pairs plus the combinatoric fake pairs. The numbers of combinatoric pairs are

$$\begin{aligned} N^{+-}_{fake} &= (N_{\pi+}q_\pi + N_{\mathrm{K}+}q_\mathrm{K})(N_{\pi-}q_\pi + N_{\mathrm{K}-}q_\mathrm{K}) \\ N^{++} &= N^2_{\pi+}q^2_\pi/2 + N_{\pi+}N_{\mathrm{K}+}q_\pi q_\mathrm{K} + N^2_{\mathrm{K}+}q^2_\mathrm{K}/2 \\ N^{--} &= N^2_{\pi-}q^2_\pi/2 + N_{\pi-}N_{\mathrm{K}-}q_\pi q_\mathrm{K} + N^2_{\mathrm{K}-}q^2_\mathrm{K}/2. \end{aligned} \tag{13}$$

(The terms $N(N-1)q^2/2 \approx N^2q^2/2$ arise from the combinatorics of pairing identical particles without double counting.) Further assume that $N_{\pi+} = N_{\pi-}$, but that $N_{\mathrm{K}+} \neq N_{\mathrm{K}-}$. Then like-sign subtraction *almost* recovers the true signal,

$$N^{+-} - N^{++} - N^{--} = \boxed{N_{\mu\mu}} - (N_{\mathrm{K}+} - N_{\mathrm{K}-})^2 q^2_\mathrm{K}/2, \tag{14}$$

except for the asymmetry in kaon abundance. Unequal K^+ and K^- yields are well established at AGS energies [9], but the asymmetry should be much smaller in the central rapidity region at RHIC. It may be possible to correct for the residual background with

a Monte Carlo simulation to derive the true signal, $N_{\mu\mu}$. Note that $N_{\mu\mu} \propto N_\pi$ has been assumed, and that $N^{+-}_{fake} \propto N^2_\pi$, so the combinatoric background problem worsens proportionally to the event multiplicity.

In conclusion,

- a soft muon spectrum hurts because the muons range out, killing the muon detection efficiency at low energy, and because soft muons suffer moderate to severe energy loss straggling and multiple coulomb scattering, which harm invariant mass resolution;
- in order to provide a low muon kinetic energy threshold and to preserve invariant mass resolution, low atomic number (Z) absorber materials (like Be and C) must be used, and these requirements are incompatible with traditional calorimeter materials like Fe, Cu, Pb, or U;
- even though muon candidates must penetrate $\sim 7\lambda$ in order to eliminate sail-through hadrons and shower products, to preserve resolution, the muon momentum measurement should be made after the least thickness of absorber necessary ($\sim 4\lambda$); this increases the difficulty of tracking because of the large number of extraneous particles, and requires a second absorber downstream to complete muon identification;
- the accompanying soft hadron spectrum in not very time-dilated, and pions and kaons have a significant likelihood of decaying into background muons before they interact in the absorber;
- the $\pi \rightarrow \mu\nu$ background cannot be eliminated by tracking through an absorber, because the muon angle and momentum distributions overlap the parent pion angle and momentum too closely;
- with sufficient statistics, a like-sign subtraction and Monte Carlo correction may allow a direct muon pair spectrum to be seen even with a modest signal to background ratio.

The author acknowledges many insightful suggestions by Glenn Young that helped guide this work. The author also thanks Tim Fox, an undergraduate summer student at ORNL in 1989, for his help with GEANT Monte Carlo studies. This research was supported by the Division of High Energy and Nuclear Physics, U.S. Department of Energy, under contract DE-AC05-84OR21400 with Martin Marietta Energy Systems, Inc.

References

[1] K. Bunnell *et al.*, Phys. Rev. Lett. **40**, 136 (1978).

[2] G. Roche *et al.*, Phys. Rev. Lett. **61**, 1069 (1988).

[3] RHIC R&D Proposal 10, "Calorimeter/Absorber Optimization for the RHIC Dimuon Experiment," S. Aronson *et al.*, Brookhaven National Laboratory, Sept. 1988.

[4] GEANT3, R. Brun *et al.*, CERN DD Division, Geneva, Switzerland, 1987.

[5] Particle Data Group, C.G. Wohl *et al.*, Rev. Mod. Phys. **56**, No. 2, Part II, S48-S60 (1984).

[6] CRC Handbook of Chemistry and Physics, Robert C. Weast, Ed., pp. B-1 – B-160, 56^{th} Edition, CRC Press, Cleveland, Ohio, 1975.

[7] private communication, Brush Wellman Inc., Elmore OH, 419-862-2745, and Brush Wellman Inc., Tucson, AZ, 602-746-0251, 1989.

[8] private communication, Union Carbide Inc., 800-342-3698, 1989.

[9] T. Abbott *et al.*, Phys. Rev. Lett. **64**, 847 (1990).

1 Tables

Table 1: Properties of 31 low-Z absorber candidates are listed, including the density ρ, radiation length X_0, hadronic interaction length λ, and ratios of X_0/λ.

Table 2: Further properties of 31 low-Z absorber candidates are listed, including the range R of a 2000 MeV (K.E.) muon, energy loss ΔE of a 2000 MeV muon penetrating 9λ of absorber, the mean MCS angle θ_{MCS} of a 2000 MeV muon, and the probabilities P(π) and P(K) for a 2000 MeV π or K meson to decay to a muon before interacting in 9λ of absorber.

2 Figures

Figure 1: The average ranges of muons, in interaction length units, as a function of muon kinetic energy, for three absorber materials: beryllium (Be), carbon (C), and copper (Cu).

Figure 2: The exponentially decreasing probabilities that a hadron can sail through an absorber just thick enough to range out muons of a given kinetic energy. To reduce the probability to $\leq 10^{-3}$ in a Be absorber, muons must have kinetic energy > 900 MeV, in a C absorber, K.E. > 1100 MeV, and in Cu, K.E. > 1450 MeV.

Figure 3: Energy loss straggling (ELS) histograms of $|p_{peak} - p_{exit}|/|p_{peak}|$ for 1500 Monte Carlo muons of 2000 MeV K.E. incident on three absorbers: 4.5λ Be, 3.9λ C, and 2.9λ Cu. The histograms were smoothed to compensate for low statistics.

Figure 4: Muon exit angle distributions due to multiple coulomb scattering (MCS) for the same Monte Carlo muons in the same three absorbers as in Fig. 3. The histograms were smoothed to compensate for low statistics.

Figure 5: The fractional invariant mass resolution $\Delta M/M$ for two cases of invariant mass (ρ meson, mass 770 MeV, and ψ meson, 3100 MeV), and three absorbers (4.5λ Be, 3.9λ C, and 2.9λ Cu), for meson kinetic energies ranging from 1 to 19 GeV. The fractional resolution in all cases is below 0.12, and in all but one case less than the fractional intrinsic width of the ρ, 0.085.

Figure 6: The probabilities (on a log scale) for π and K mesons to decay to muons for the range of meson kinetic energies 0 – 20000 MeV. The four curves correspond to kaons in a Be absorber, kaons in Cu, pions in Be, and pions in Cu. The probabilities are not drawn at low meson kinetic energy (on the left) because the muons resulting from the decay of such mesons have too little energy to penetrate a $\sim 7\lambda$ absorber.

Figure 7: The probability distributions of muon lab kinetic energy for six cases: $\pi \rightarrow \mu\nu$ for 2000, 5000, and 10000 MeV K.E. pions, and $K \rightarrow \mu\nu$ for 2000, 5000, and 10000 MeV K.E. kaons. The probabilities are uniformly distributed between $E'_{min} - m_\mu$ and $E'_{max} - m_\mu$, as explained in the text following Eq. (9).

Figure 8: The probability distributions of lab angle between parent pion and daughter muon for three cases: $\pi \rightarrow \mu\nu$ for 2000, 5000, and 10000 MeV K.E. pions. The distributions are (integrably) singular at the angle given by Eq. (10).

Figure 9: The probability distributions of lab angle between parent kaon and daughter muon for three cases: $K \rightarrow \mu\nu$ for 2000, 5000, and 10000 MeV K.E. kaons. Note that the angle scale is much larger for kaons than for pions (Fig. 8).

Light Materials Properties – I

Compound	ρ ($\frac{g}{cm^3}$)	X_0 ($\frac{g}{cm^2}$)	X_0 (cm)	λ ($\frac{g}{cm^2}$)	λ (cm)	$\frac{X_0}{\lambda}$ ($\frac{g}{cm^3}$)	$\frac{X_0}{\lambda}$
Li	0.534	82.05	153.65	72.8	136.3	0.60	1.13
LiH	0.82	78.7	96.0	69.0	84.2	0.93	1.14
LiD	0.92 (?)	88.6	96.3	67.4	73.3	1.21	1.31
Li_2C_2	1.65	51.8	31.4	79.6	48.2	1.07	0.651
Li_2CO_3	2.11	39.9	18.9	86.1	40.8	0.98	0.463
$Li_2C_2O_4$	2.12	39.2	18.5	86.6	40.9	0.96	0.453
LiOH	1.46	42.1	28.9	82.5	56.5	0.75	0.510
$LiNO_3$	2.38	37.2	15.6	88.4	37.2	1.00	0.421
Li_2O	2.01	46.95	23.3	81.7	40.65	1.16	0.575
Li_3N	?	56.0		78.2			0.716
Be	1.848	65.3	35.3	75.3	40.7	1.60	0.867
Be_2C	1.90	53.9	28.35	78.6	41.4	1.30	0.686
BeO	3.01	41.3	13.7	84.9	28.2	1.46	0.486
Be_3N_2	?	47.8		81.2			0.589
$Be_{.62}Al_{.38}$	?	30.9		92.8			0.333
B	2.37	52.7	22.2	81.6	34.4	1.53	0.646
B_4C	2.52	50.1	19.9	82.2	32.6	1.54	0.609
BN	2.25	43.25	19.2	85.1	37.8	1.14	0.508
B_2O_3	2.46	38.4	15.6	88.1	35.8	1.07	0.436
$LiBH_4$	?	61.3		70.95			0.864
C (graphite) (diamond)	2.265 3.51	42.7 "	18.85 12.2	84.1 "	37.15 24.0	1.15 1.78	0.508 "
MgO_2	?	29.55		96.1			0.307
Al	2.70	24.0	8.89	106.3	39.4	0.61	0.226
AlB_{12}	2.55	43.7	17.1	85.0	33.3	1.31	0.514
AlB_2	3.19	31.7	9.93	93.7	29.4	1.08	0.338
Al_4C_3	2.36	27.0	11.4	99.7	42.3	0.64	0.271
AlN	3.26	27.5	8.42	99.2	30.4	0.90	0.277
Al_2O_3	3.97	27.9	7.04	98.7	24.9	1.12	0.283
Fe	7.87	13.8	1.76	131.2	16.7	0.83	0.105
Cu	8.96	12.9	1.44	136.2	15.2	0.85	0.0947

Table 2

Light Materials Properties – II

Compound	R_{2000} (cm) range of a 2000-MeV μ	R_{2000} (λ)	$\Delta E_{9\lambda}$ (MeV) energy loss of μ in 9 λ at 2000 MeV	$\frac{dE}{dx}$ $(\frac{MeV}{g/cm^2})$ 1st g/cm^2 of 2000-MeV μ	θ_{MCS} (rad) 2000-MeV μ into 9 λ	P(π)	P(K)
						2000-MeV π/K: prob to decay to μ in 9 λ	
Li	2130	15.6	1160	1.815	0.032	$1.19 \cdot 10^{-2}$	$4.55 \cdot 10^{-2}$
LiH	1205	14.3	1250	2.074	0.033	$7.44 \cdot 10^{-3}$	$2.92 \cdot 10^{-2}$
LiD	1209	16.5	1090	1.842	0.028	$6.43 \cdot 10^{-3}$	$2.54 \cdot 10^{-2}$
Li_2C_2	657	13.6	1320	1.906	0.048	$4.30 \cdot 10^{-3}$	$1.71 \cdot 10^{-2}$
Li_2CO_3	508	12.5	1440	1.934	0.063	$3.66 \cdot 10^{-3}$	$1.46 \cdot 10^{-2}$
$Li_2C_2O_4$	502	12.3	1460	1.947	0.065	$3.67 \cdot 10^{-3}$	$1.47 \cdot 10^{-2}$
LiOH	703	12.4	1440	2.016	0.060	$5.07 \cdot 10^{-3}$	$2.01 \cdot 10^{-2}$
$LiNO_3$	448	12.0	1490	1.947	0.070	$3.35 \cdot 10^{-3}$	$1.34 \cdot 10^{-2}$
Li_2O	551	13.6	1430	1.867	0.051	$3.63 \cdot 10^{-3}$	$1.45 \cdot 10^{-2}$
Li_3N		14.1	1280	1.880	0.044		
Be	626	15.4	1170	1.780	0.037	$3.60 \cdot 10^{-3}$	$1.44 \cdot 10^{-2}$
Be_2C	583	14.1	1280	1.863	0.045	$3.68 \cdot 10^{-3}$	$1.47 \cdot 10^{-2}$
BeO	365	12.9	1390	1.881	0.059	$2.53 \cdot 10^{-3}$	$1.02 \cdot 10^{-2}$
Be_3N_2	549*	13.5	1330	1.882	0.051		
$Be_{.62}Al_{.38}$		12.1	1490	1.868	0.080		
B	475	13.8	1300	1.834	0.047	$3.07 \cdot 10^{-3}$	$1.23 \cdot 10^{-2}$
B_4C	440	13.5	1330	1.860	0.050	$2.91 \cdot 10^{-3}$	$1.17 \cdot 10^{-2}$
BN	480	12.7	1410	1.916	0.059	$3.39 \cdot 10^{-3}$	$1.36 \cdot 10^{-2}$
B_2O_3	437	12.2	1470	1.927	0.067	$3.22 \cdot 10^{-3}$	$1.29 \cdot 10^{-2}$
$LiBH_4$		12.9	1390	2.247	0.043		

Table 2 cont.

Light Materials Properties – II

Compound	R_{2000} (cm) range of a 2000-MeV μ	R_{2000} (λ)	$\Delta E_{9\lambda}$ (MeV) energy loss of μ in 9 λ at 2000 MeV	$\frac{dE}{dx}$ $(\frac{MeV}{g/cm^2})$ 1st g/cm^2 of 2000-MeV μ	θ_{MCS} (rad) 2000-MeV μ into 9 λ	P(π)	P(K)
						2000-MeV π/K: prob to decay to μ in 9 λ	
C (graphite)	462	12.4	1440	1.977	0.060	$3.34 \cdot 10^{-3}$	$1.34 \cdot 10^{-2}$
(diamond)	302	12.6	1420	1.944	0.059	$2.15 \cdot 10^{-3}$	$8.70 \cdot 10^{-2}$
MgO_2		11.1	1620	1.977	0.099		
Al	421	10.7	1670	1.850	0.129	$3.58 \cdot 10^{-3}$	$1.43 \cdot 10^{-2}$
AlB_{12}	441	13.2	1360	1.840	0.056	$2.98 \cdot 10^{-3}$	$1.20 \cdot 10^{-2}$
AlB_2	358	12.2	1470	1.822	0.078	$2.64 \cdot 10^{-3}$	$1.06 \cdot 10^{-2}$
Al_4C_3	472	11.2	1600	1.881	0.104	$3.83 \cdot 10^{-3}$	$1.53 \cdot 10^{-2}$
AlN	343	11.3	1580	1.869	0.099	$2.76 \cdot 10^{-3}$	$1.11 \cdot 10^{-2}$
Al_2O_3	281	11.3	1580	1.867	0.097	$2.26 \cdot 10^{-3}$	$9.08 \cdot 10^{-3}$
Fe	157	9.41	1880	1.711	>0.20	$1.54 \cdot 10^{-3}$	$6.24 \cdot 10^{-3}$
Cu	142	9.34	1900	1.670	>0.20	$1.41 \cdot 10^{-3}$	$5.70 \cdot 10^{-3}$

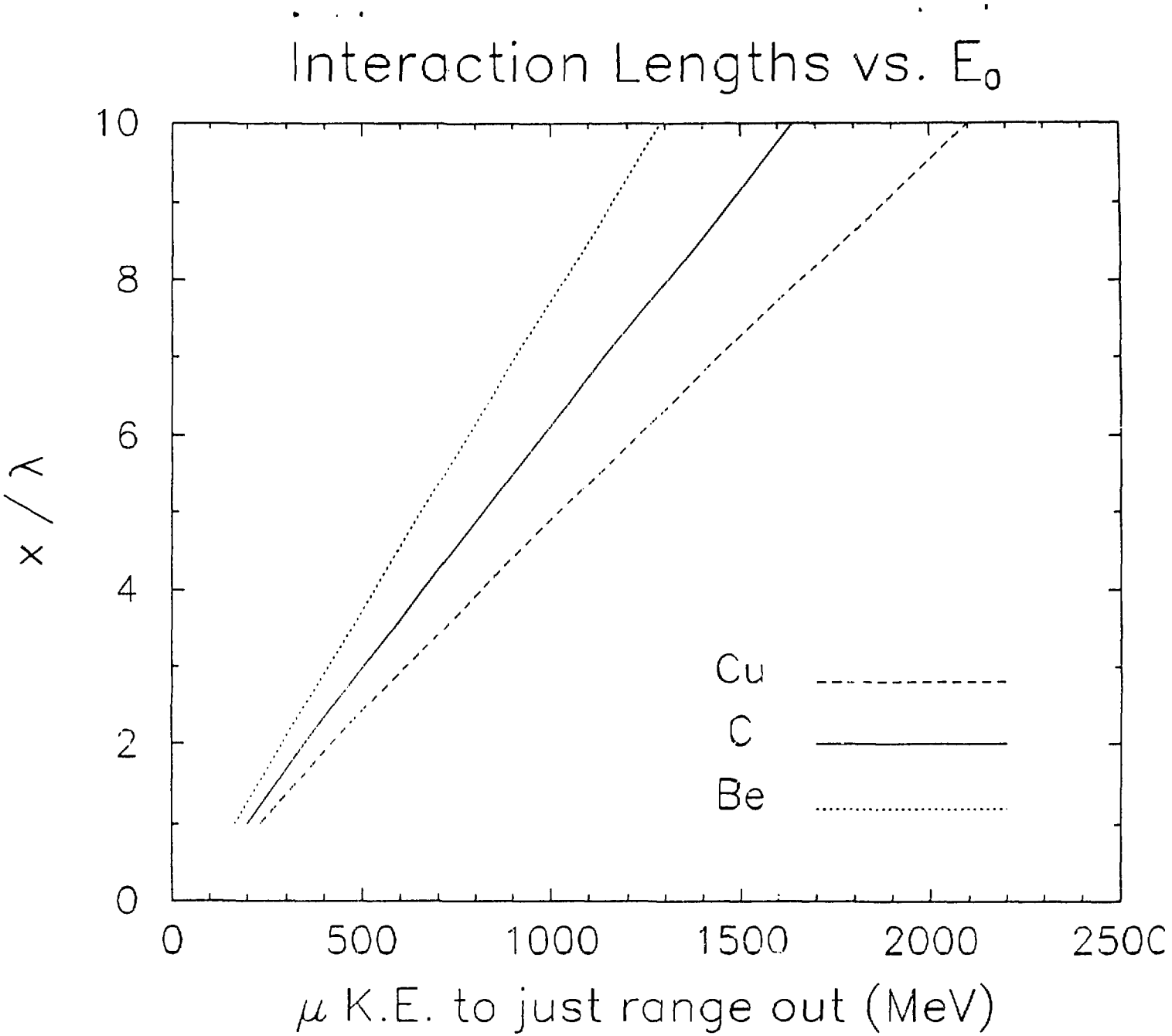
Interaction Lengths vs. E_0
10
8
6
4
2
0
x / λ
0
500
1000
1500
2000
2500
μ K.E. to just range out (MeV)
Cu
C
Be

Fig. 1

Fig. 2

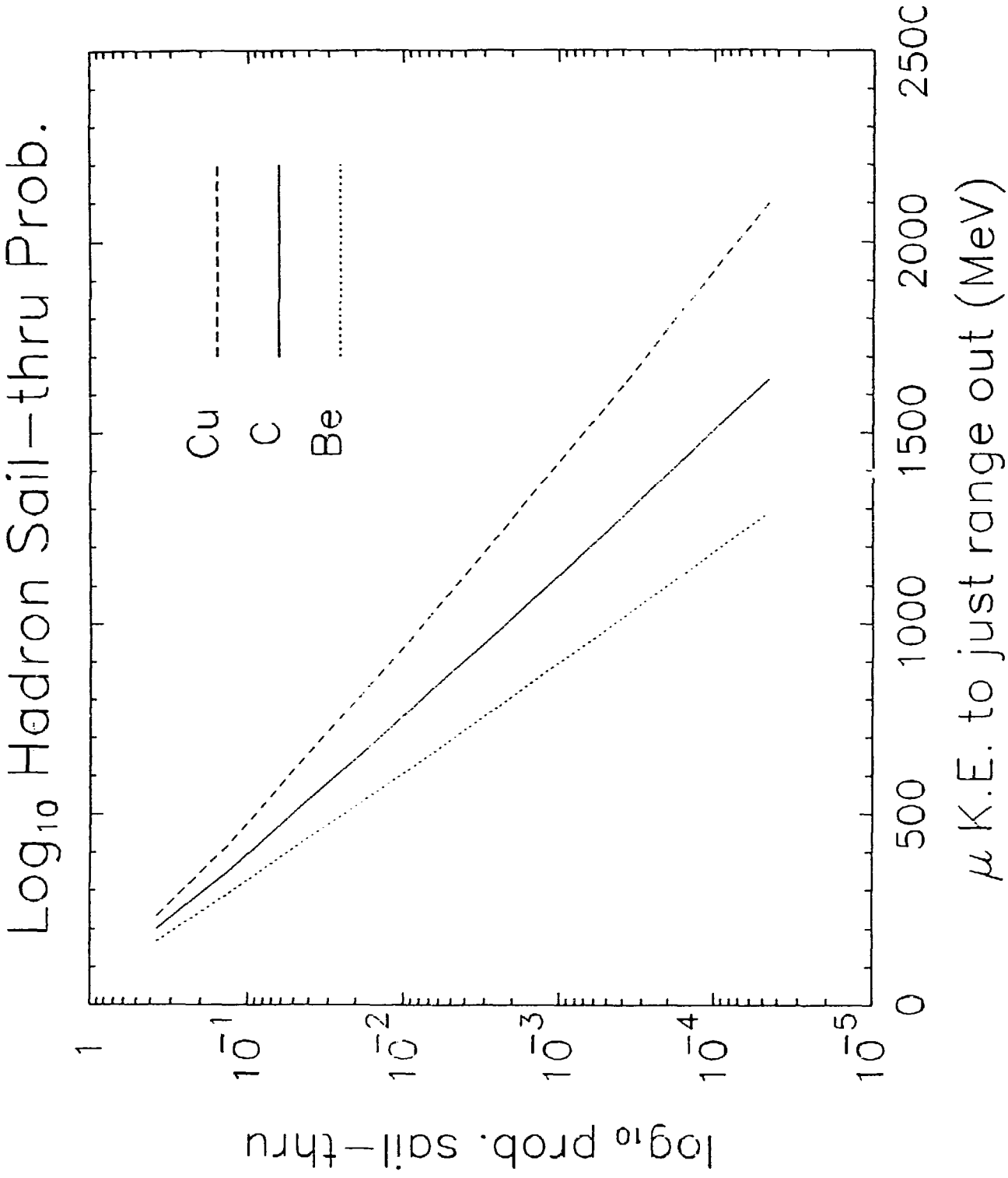
Log10 Hadron Sail-thru Prob.
Cu
C
Be
log10 prob. sail-thru
1
10^-1
10^-2
10^-3
10^-4
10^-5
0
500
1000
1500
2000
2500
μ K.E. to just range out (MeV)

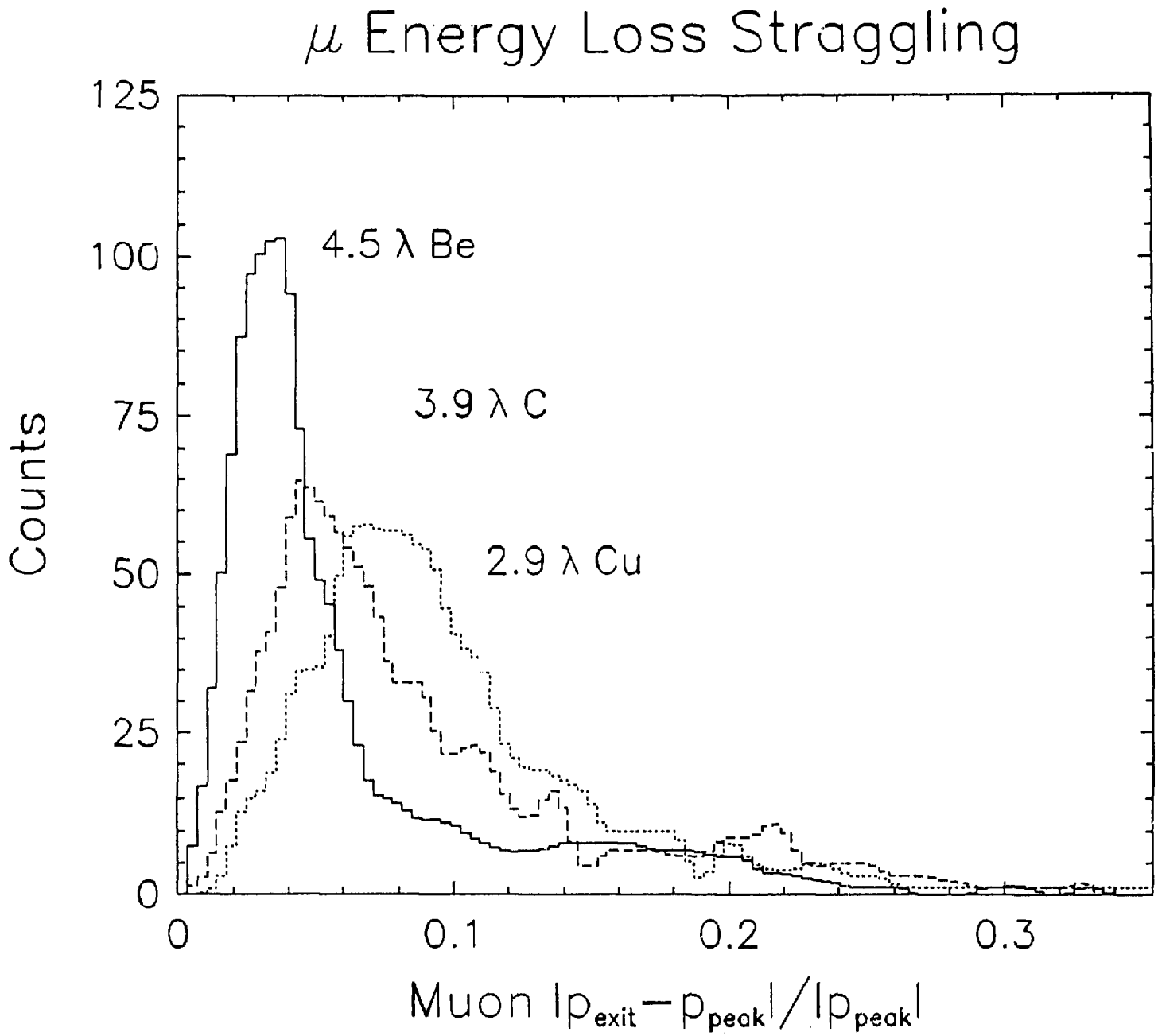
μ Energy Loss Straggling
125
100
75
50
25
0
Counts
4.5 λ Be
3.9 λ C
2.9 λ Cu
0
0.1
0.2
0.3
Muon |p_exit − p_peak| / |p_peak|

Fig. 3

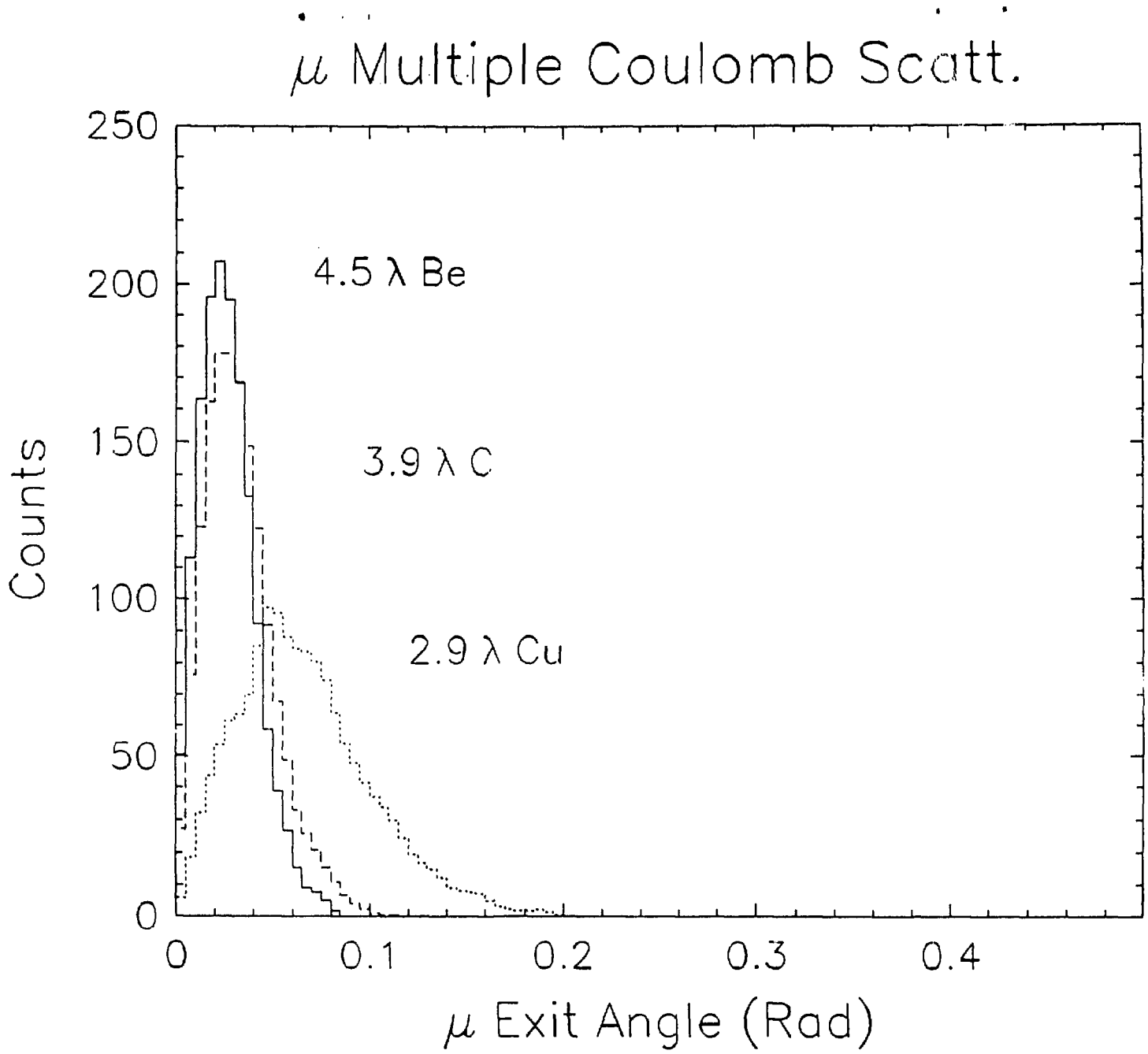
μ Multiple Coulomb Scatt.
250
200
150
100
50
0
Counts
4.5 λ Be
3.9 λ C
2.9 λ Cu
0
0.1
0.2
0.3
0.4
μ Exit Angle (Rad)

Fig. 4

Fig. 5

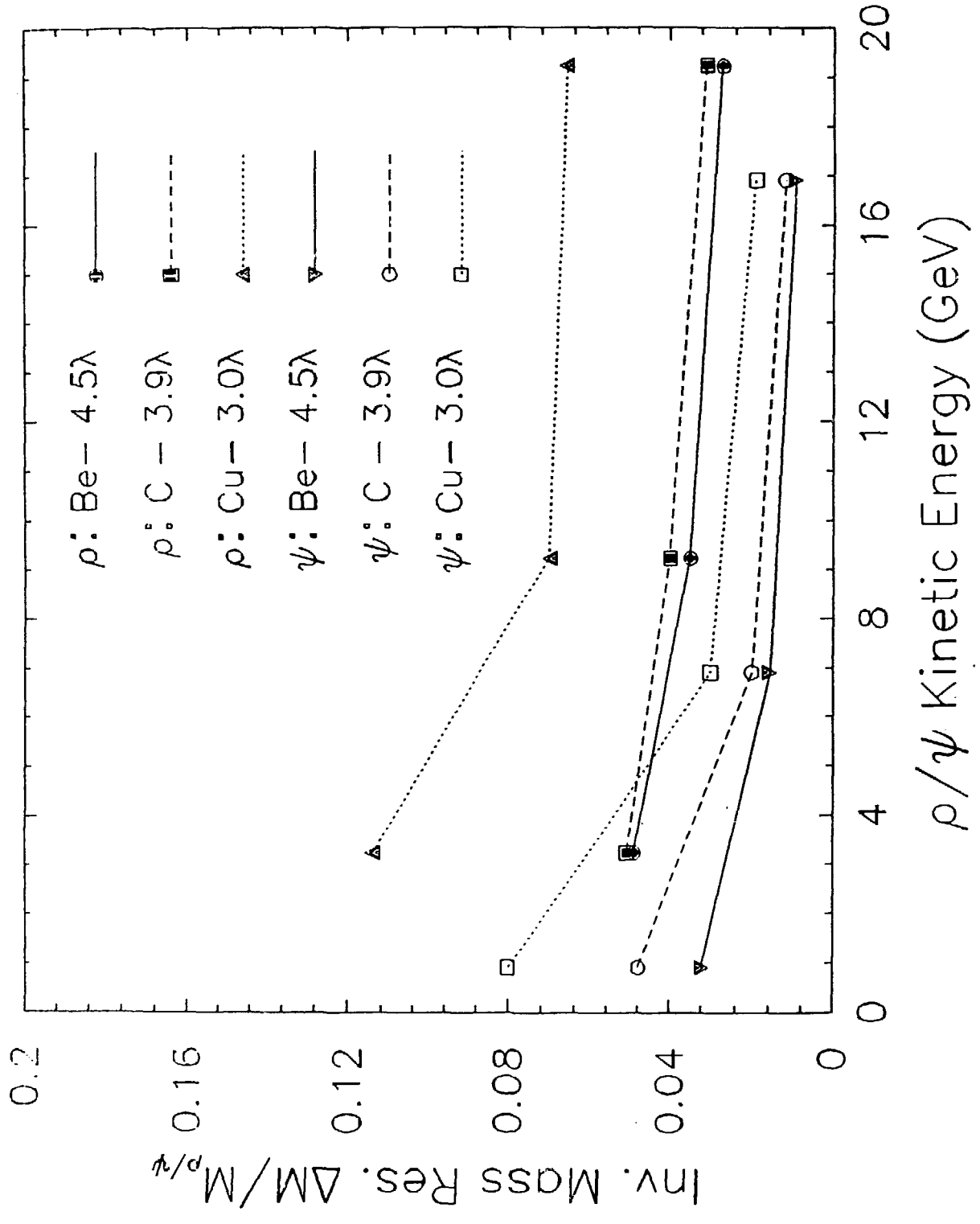
GEANT μ M.C.S. and E. Straggling
ρ: Be– 4.5λ
ρ: C – 3.9λ
ρ: Cu– 3.0λ
ψ: Be– 4.5λ
ψ: C – 3.9λ
ψ: Cu– 3.0λ
Inv. Mass Res. ΔM/M ρ/ψ
0
0.04
0.08
0.12
0.16
0.2
0
4
8
12
16
20
ρ/ψ Kinetic Energy (GeV)

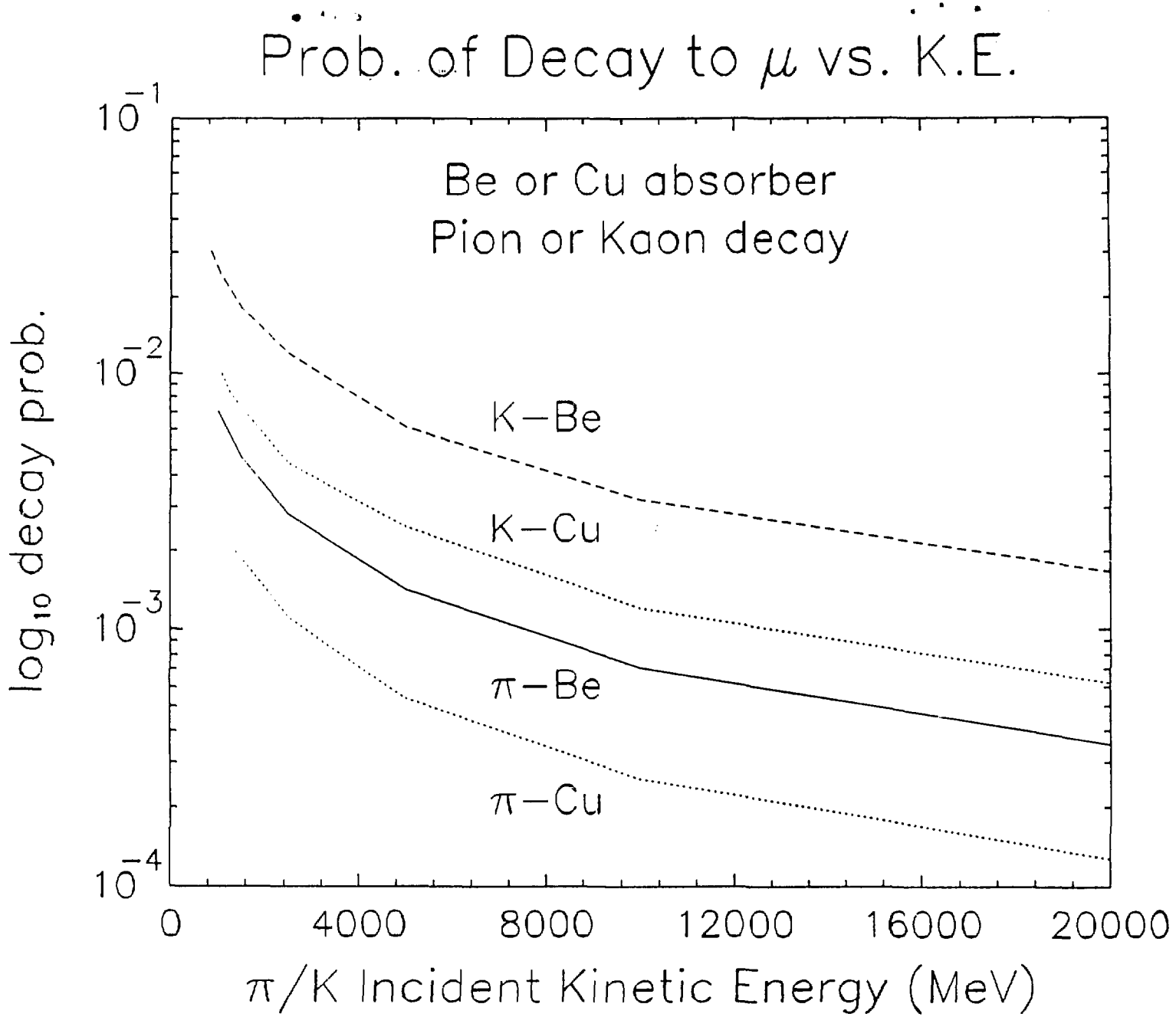
Prob. of Decay to μ vs. K.E.
Be or Cu absorber
Pion or Kaon decay
K−Be
K−Cu
π−Be
π−Cu
log10 decay prob.
10−1
10−2
10−3
10−4
0
4000
8000
12000
16000
20000
π/K Incident Kinetic Energy (MeV)

Fig. 6

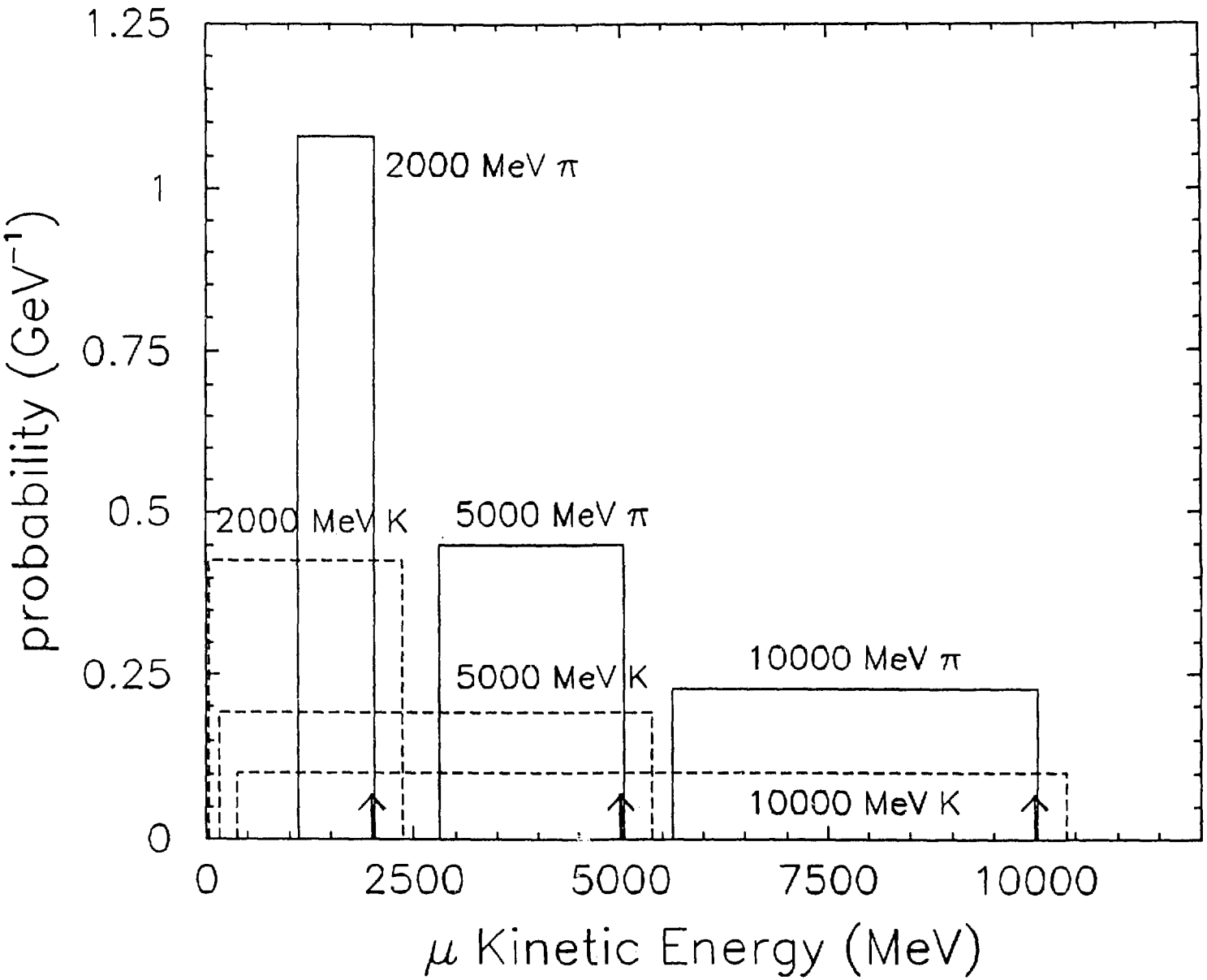
π;K → μν Decay
1.25
1
0.75
0.5
0.25
0
probability (GeV⁻¹)
2000 MeV π
2000 MeV K
5000 MeV π
5000 MeV K
10000 MeV π
10000 MeV K
0
2500
5000
7500
10000
μ Kinetic Energy (MeV)

Fig. 7

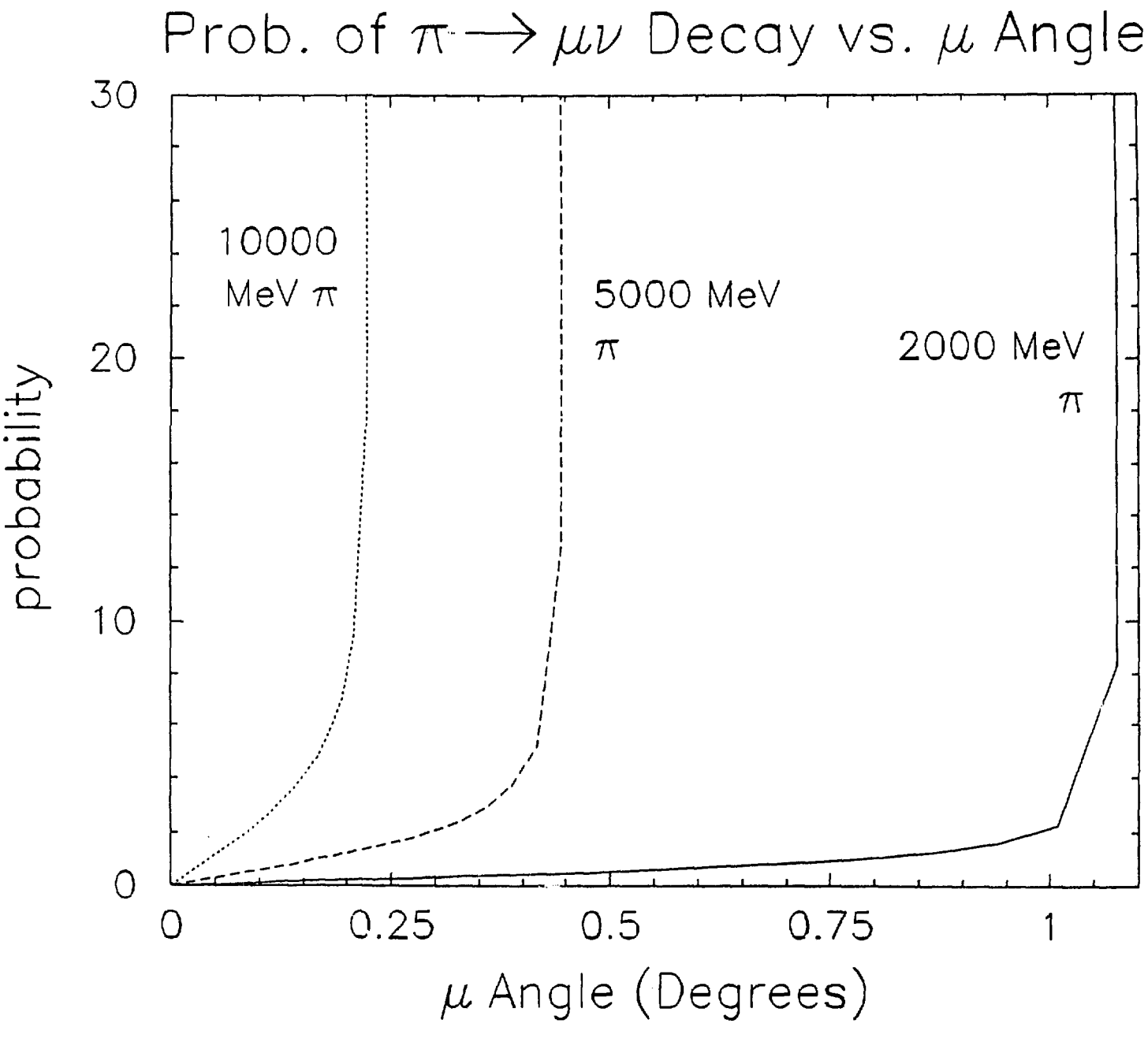
Prob. of $\pi \rightarrow \mu\nu$ Decay vs. μ Angle
probability
30
20
10
0
0
0.25
0.5
0.75
1
μ Angle (Degrees)
10000 MeV π
5000 MeV π
2000 MeV π

Fig. 8

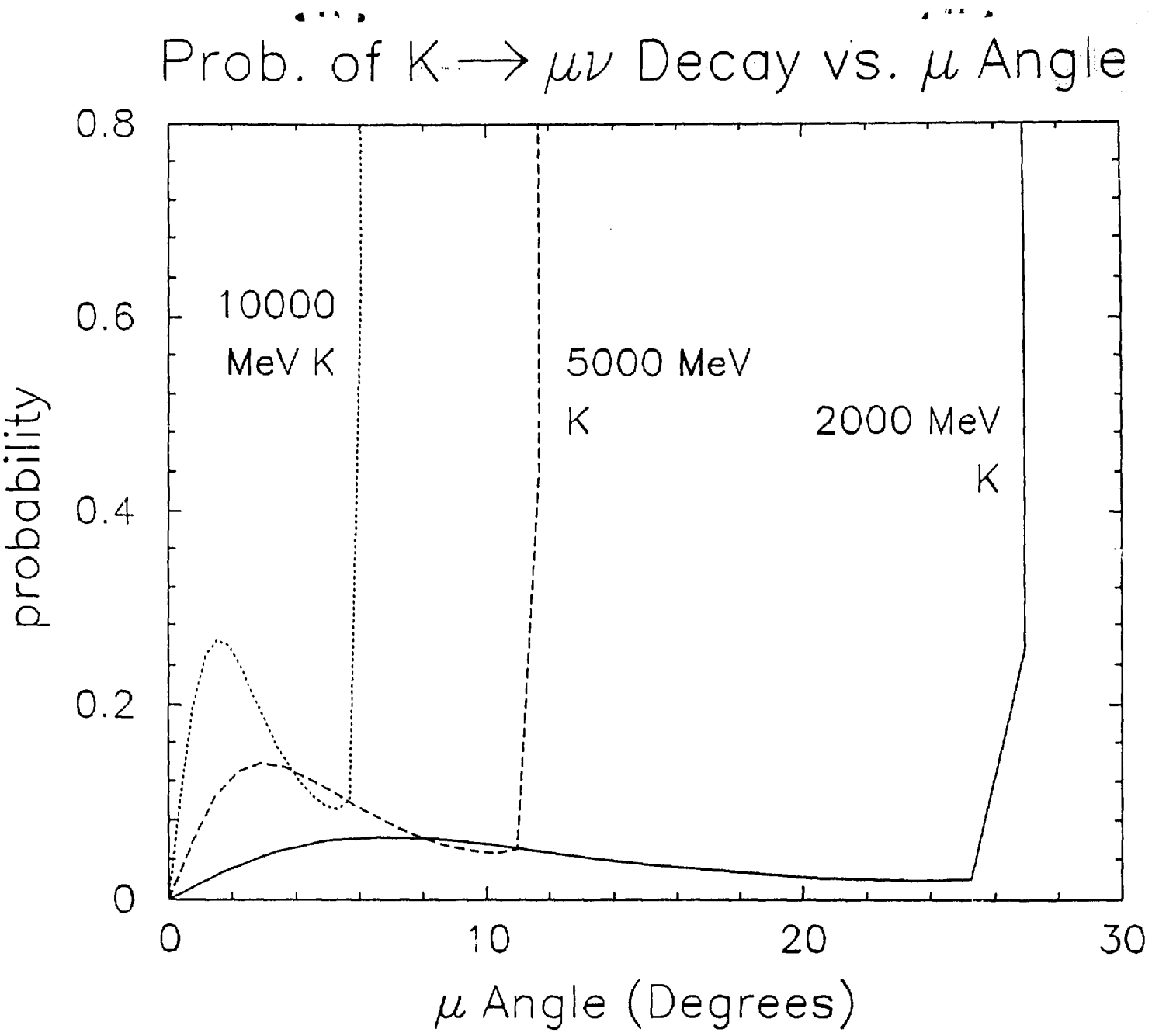
Prob. of K → μν Decay vs. μ Angle
probability
0.8
0.6
0.4
0.2
0
10000
MeV K
5000 MeV
K
2000 MeV
K
0
10
20
30
μ Angle (Degrees)

Fig. 9